MODELING FLOOD SHOCK WAVE PROPAGATION WITH THE SMOOTHED PARTICLE HYDRODYNAMICS (SPH) METHOD: AN EXPERIMENTAL COMPARISON STUDY

TURHAN, E.[1*] – OZMEN-CAGATAY, H.[2] – TANTEKIN, A.[3]

[1]*Department of Civil Engineering, Adana Science and Technology University 01250 Adana, Turkey*

[2]*Department of Civil Engineering, Cukurova University, 01330 Adana, Turkey*

[3]*Department of Mechanical Engineering, Adana Science and Technology University 01250 Adana, Turkey*

**Corresponding author*
e-mail: eturhan@adanabtu.edu.tr; phone: +90-322-455-0000; fax: +90-322-455-0009

(Received 30th Nov 2018; accepted 4th Feb 2019)

Abstract. The applicability of experimental and numerical models used for the solution of dam-break flows is vital for better dam projects and also in preventing related accidents. The high cost and the time-consuming nature of laboratory studies require consistency in the investigation of numerical models. In this study, the propagation of a flow using a fluid with a different density from that of normal water in the reservoir was investigated both experimentally and numerically. Salt water was preferred as a Newtonian fluid in order to observe the propagation of flows in different density after a sudden break. A small-scale channel was constructed and laboratory data were obtained using image processing techniques. For the numerical model, Smoothed-Particle Hydrodynamics (SPH) method and Reynolds Averaged Navier-Stokes (RANS) equations solved by Flow-3D software, were applied. Flow depth changes were observed in the reservoir and the downstream. The data obtained from all methods were compared with each other. The results of two numerical simulations point out that the disagreements on graphs in the time evolutions of the fluid levels in the SPH increase due to turbulence effects, whilst, these differences decrease in the RANS equations solved by Flow-3D software. Consequently, since the SPH provides taking the measures and developing intervention strategies to reduce the risks connected to the evolution of dam-break flows, it is thought that future validation studies of the model will be require with the use of data observed in this field.

Keywords: *dam-break, density effect, image processing, particle method, volume of fluid*

Introduction

Some environmental flows can be simulated like dam-break induced shock waves. The prediction of these flows is one of required elements in the design of a dam. Dams are constructed for specific purposes such as water supply, flood control, irrigation, navigation, sedimentation control and hydropower (Lee et al., 2018). Past examples show us that the dams can be destroyed due to various reasons. The reasons of failure can be different for each dam and each case. While rockfill dams usually fail after a certain amount of time elapses, concrete dams fail a lot more suddenly. In practice the release of dam-break flows will be more gradual than this idealization. However, the sudden release may be expected to give the worst scenario. The shock wave propagation, caused by a dam-break, produces damaging effects in the downstream. It can be seen common that the propagation of water mixture which of different density from water can be formed in the downstream after torrential rain or a dam collapse. Hence, the flood wave can damage both living species and the environment (Yenigun et

http://www.aloki.hu ● ISSN 1589 1623 (Print) ● ISSN 1785 0037 (Online)
DOI: http://dx.doi.org/10.15666/aeer/1702_30333047
© 2019, ALÖKI Kft., Budapest, Hungary

al., 2016). For the process of the dam construction and the evaluation of a demolition situation after the construction, it is important to simulate the flow characteristics on a dam-break problem with laboratory experiments and numerical models. Various dam-break flow problems, which use water as the fluid in the reservoir, was experimentally and numerically examined in the literature. Ritter was the first to examine this flow problem in 1892. He used Saint-Venant equations to solve the sudden dam-break problem in a horizontal, rectangular, frictionless channel and he considered the downstream as a dry bed and the reservoir in an infinite length (Vischer and Hager, 1998; Chanson, 2005). There are numerous studies investigating a dry and/or wet bed downstream (Stoker, 1957; Bellos et al., 1992; Mohapatra and Bhallamudi, 1996; Stansby, 1998; Janosi et al., 2004; Bukreev and Gusev, 2005; Gao et al., 2010; Oertel and Bung, 2012; Ozmen-Cagatay et al., 2014; Kocaman and Ozmen-Cagatay, 2015; Turhan, 2017; Turhan et al., 2019). It is possible to see many studies in which dam-break flow problem has been examined experimentally using image processing techniques in the literature. (Spinewine and Zech, 2007; Ozmen-Cagatay and Kocaman, 2010; Aureli et al., 2011; Yang et al., 2011; Kocaman and Ozmen-Cagatay, 2012; Lobovsky et al., 2013; Kunugi et al., 2013; Albano et al., 2014; Aureli et al., 2014; Amaral et al., 2016; Hui et al., 2017; Liu, 2018). There are a limited number of studies that include different density Newtonian fluids in the reservoir (Janosi et al., 2004; Ancey and Cochard, 2009; Shakibaeini and Jin, 2011; Li et al., 2013; Furuya et al., 2014). Concerning the research in this flow problem, using salt water as a Newtonian fluid in a dry channel in rapidly unsteady flow can be interpreted an original study. Since laboratory experiments are costly and time-consuming processes, using software program to solve these problems is essential (Karaer et al., 2018). With recent developments in computer technology, using particle methods has become more widespread and also, their sensitivity in modeling applications requires further testing. There are several software programs in which the dam-break flow problem is numerically simulated. In this study, Smoothed-Particle Hydrodynamics (SPH) method used as a particle method and it was first developed by Gingold and Monaghan (1977), Lucy (1977), Liu and Liu (2003) for astrophysical problems. Subsequently, it has been applied to various problems in fluid dynamics (Dalrymple and Rogers, 2006; Gomez-Gesteira et al., 2012; Dominguez et al., 2013; Crespo et al., 2015; Gu et al., 2017).

Dam-break shock waves usually affect large downstream regions and the common tendency is to comment flow characteristics in the horizontal scale rather than along the flow depth (Miao et al., 2011; Luo et al., 2017; Akbari, 2018). Recently, due to the increase in computer technology, Flow-3D, which is computational fluid dynamics (CFD) software based on volume of fluid (VOF) method, has been used widely to analyze free-surface flows among the other commercially available software programs (An et al., 2012; Ozmen-Cagatay et al., 2014; Robb and Vasquez, 2015; Hu et al., 2018). In the literature, the SPH model was applied to predict a dam-break flood propagation, which might occur in a specific living area. The studies in the literature represents the significant potentials of numerical and laboratory modeling in practical engineering applications. Moreover, the results obtained from all methods assisted to validate the results of each other in terms of SPH, RANS and laboratory experiments. (Chen et al., 2005; Albano et al., 2016; Gu et al., 2017; Xie et al., 2017).

In this paper, the sudden dam-break flow propagation of a different density Newtonian fluid in a small-scale, rectangular and horizontal channel was experimentally and numerically investigated. The purpose of this study is to model the flow movement

http://www.aloki.hu ● ISSN 1589 1623 (Print) ● ISSN 1785 0037 (Online)
DOI: http://dx.doi.org/10.15666/aeer/1702_30333047
© 2019, ALÖKI Kft., Budapest, Hungary

in an idealized dam-break configuration in case of a Newtonian fluid in the reservoir. Normal water is a Newtonian fluid which of that the dynamic viscosity value is 0.001 kg/m.s and density value is 1000 kg/m^3 at the constant temperature of T_0 = 23.7 °C. Salt water was preferred as a Newtonian fluid to investigate the effect of a fluid with a different density to normal water. Thus, the behavior of a high density fluid has been tried to be analyzed. Experimental data were digitized using image processing techniques. Fluid free-surface profile graphs and snapshots were obtained at four downstream locations and at various specified distances in the reservoir and downstream. The SPH method and RANS equations, solved by the Flow-3D software program, were employed for the numerical models. The results obtained from the SPH were compared to laboratory experiments and RANS equations solutions.

Materials and methods

Experimental set-up

The reservoir and the downstream lengths of the rectangular and horizontal channel, in which the experiments employed, were designed to be 0.30 m and 0.916 m, respectively, as can be seen in *Figure 1*. In order to observe the sudden and unsteady flow behavior, the channel was selected in a small-scale. The channel was made of plexiglas and a gate of 0.35 m height was performed to simulate the dam-break flow problem. Furthermore, a pulley system, connected to the gate, was utilized to observe the sudden break situation. Moreover, a metal component with approximately 2 kg weight, which was attached to the hole on the gate with a rope, was designed. The rope was passed through two pulleys and it was bound to a load of about 12 kg filled with sand.

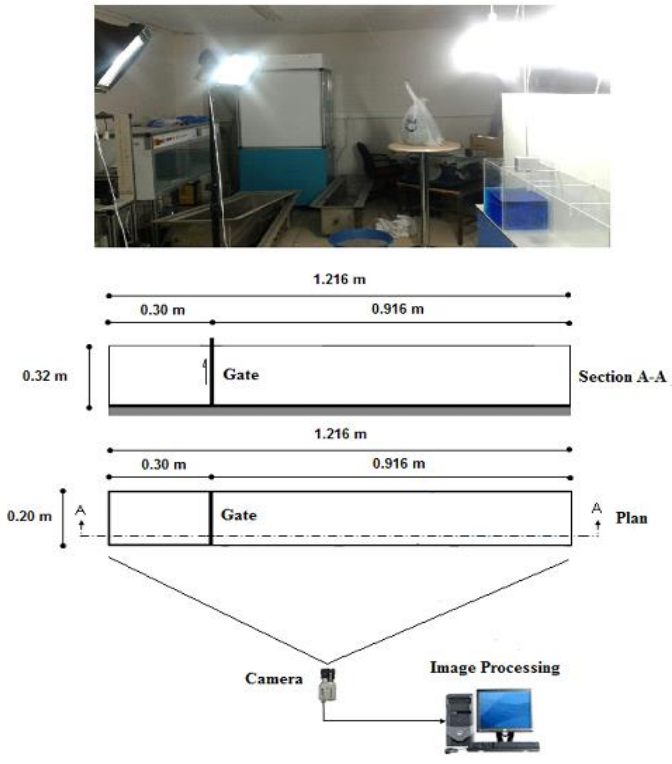

Figure 1. *Experimental set-up and gate mechanism (Turhan et al., 2018)*

http://www.aloki.hu ● ISSN 1589 1623 (Print) ● ISSN 1785 0037 (Online)
DOI: http://dx.doi.org/10.15666/aeer/1702_30333047
© 2019, ALÖKI Kft., Budapest, Hungary

The temperature of the laboratory was measured at 23.7 °C during the experiments, hence this value was used in the numerical models. The viscosity was measured to be 18 cP (0.018 kg/m.s) at this temperature with the help of a viscometer. The mixing ratio of salt water was evaluated to be 20% and a homogeneous mixture was obtained by a mixer. As a result, the fluid density was specified to be 1200 kg/m^3.

The reservoir contained salt water at a height of 0.15 m (h_o) and the downstream have a dry bed. In order to create a sudden dam-break condition, the time of gate lifting should be less than $1.25(h_o/g)^{1/2}$ (h_o: initial height and g: gravitational acceleration) as suggested by Lauber and Hager (1998). This limit value has been used in many studies (Chanson, 2005; Spinewine and Zech, 2007; Ozmen-Cagatay et al., 2014; Kocaman and Ozmen-Cagatay, 2012, 2015; Aureli et al., 2014; Turhan et al., 2019). In order to obtain approximate value of data, ten experiments were performed and the average of the values was calculated. As h_o is 0.15 m, 0.155 s becomes the limit value for sudden dam-break and in this study lifting time was under approximately 0.10 s in the video images.

Flow measurement and camera calibration

The digital image processing is produced by transferring real images to digital media in different formats such as .jpg, .bmp, .png, etc. (Yıldırım et al., 2003; Aureli et al., 2011, 2014; Liu, 2018). In this technique, as seen in *Figure 2*, the image was divided into pixels and grid view was obtained. Normal water was used as the Newtonian fluid for camera adjustments and blue food dye was preferred to provide color.

The lighting in the laboratory, where the experiment was conducted, was improved to use image processing techniques effectively before starting laboratory experiments. In order to obtain better images from the experiment, continuous lamp source of approximately 500 W was employed in the laboratory. The optimum shooting option was evaluated to be 1/125 snapshot, 85 mm, f3.5 lens and 1250 ISO proof.

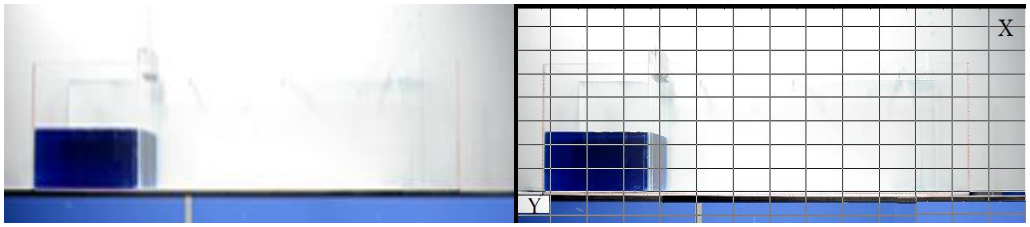

Figure 2. *Grid view in image processing (pixel)*

The frame rate and the resolution were set to 60 frames per second (fps) and 1280*720 pixels, respectively. The camera calibration process was performed with the images taken at different angles and the image distortions were eliminated. Camera shooting at the same coordinate significantly reduced the calibration error rate. The channel measurement points can be seen in *Figure 3*. Depth changes in the images were measured using a virtual wave probe (Kocaman and Ozmen-Cagatay, 2015). (x, y) coordinates were obtained by using an edge detection function at the specified locations, with the help of different colors. The simulation time and time-interval was assumed to be 3 s and approximately 0.017 (1/60 fps), respectively.

The level changes graphs are dimensionless (H-T) for all methods. For the dimensionless analysis, the values were calculated from the following equations

http://www.aloki.hu ● ISSN 1589 1623 (Print) ● ISSN 1785 0037 (Online)
DOI: http://dx.doi.org/10.15666/aeer/1702_30333047
© 2019, ALÖKI Kft., Budapest, Hungary

$T = t(g/h_o)^{1/2}$ and $H = h/h_o$ where H and T are dimensionless terms and h denotes the changes in the fluid height over time. The use of dimensionless parameters can reduce the number of variables and therefore, dimensional effect-independent assessments become possible.

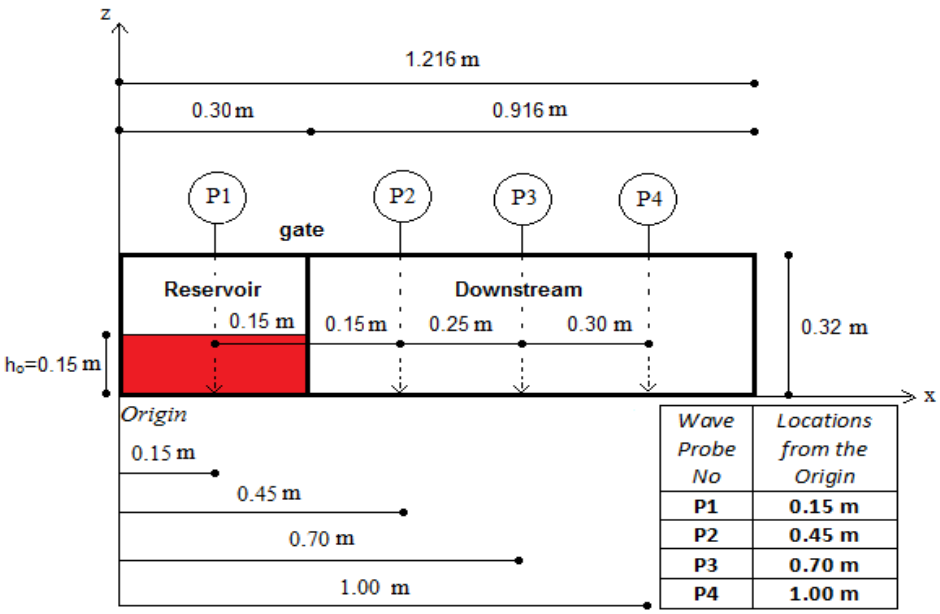

Wave Probe No	Locations from the Origin
P1	0.15 m
P2	0.45 m
P3	0.70 m
P4	1.00 m

Figure 3. *Channel measurement points*

Numerical modeling

Reynolds averaged Navier–Stokes (RANS) equations

RANS equations for an incompressible Newtonian fluid are shown in *Equations 1* and *2* (Luo et al., 2017):

$$\frac{\partial u_i}{\partial x_i} = 0 \qquad \text{(Eq.1)}$$

$$\rho \frac{\partial u_i}{\partial t} + \rho \frac{\partial (u_i u_j)}{\partial x_j} = -\frac{\partial p}{\partial x_i} + \mu \frac{\partial}{\partial x_j}\left(\frac{\partial u_i}{\partial x_j} + \frac{\partial u_j}{\partial x_i}\right) - \rho \frac{\partial \left(\overline{u_i' u_j'}\right)}{\partial x_j} + \rho g_i \qquad \text{(Eq.2)}$$

where ρ is density, u_i and u_j indicate the velocity component in the defined direction, t is time, p is pressure, μ is dynamic viscosity and g_i is gravitational force in the defined direction. When *Equation 2* is compared with the Navier–Stokes equations, it can be seen that there is an extra term, namely $\partial(\rho \overline{u_i' u_j'})/\partial x_j$ and it characterizes turbulence-induced stresses or Reynolds stresses. In the RANS equations, scalar values for all the physical properties of flow are evaluated as mean magnitudes. For laminar flow, the numbers of equation are equal to the unknown parameters. In the RANS, distinct terms have to be adjoined to the available equations. Hence, turbulence closure models are utilized to solve these problems. The term μ_t is used for turbulence viscosity, and it is found in the solution steps for the time varying RANS equations. Furthermore, the solution of this problem can be obtained with the help of many different turbulence

http://www.aloki.hu ● ISSN 1589 1623 (Print) ● ISSN 1785 0037 (Online)
DOI: http://dx.doi.org/10.15666/aeer/1702_30333047
© 2019, ALÖKI Kft., Budapest, Hungary

models (Wilcox, 2000). The k-ε turbulence model is generally preferred for the final step of the process (Kocaman and Guzel, 2011; Souders et al., 2013; Ozmen-Cagatay et al., 2014; Heydari and KhoshKonesh, 2016; Bayon et al., 2016; Ozdil et al., 2017).

The numerical solutions for the RANS were computed using Flow-3D software CFD program based on the VOF method. This program contains a mesh–grid system. It comprises a fractional area/volume obstacle representation method (FAVOR) as cell porosity technique (Flow Science Inc., 2017). All the surfaces of the channel were presumed to be smooth. The channel sidewalls were considered to be symmetric, which implies no flux and shear of any property across it. Tangential and normal velocities were accepted as zero at the solid boundary according to the no-slip condition (Rostami and Siosemarde, 2015; Kocaman and Ozmen-Cagatay, 2015). For this study, a grid size was adopted as 5 mm after executing accuracy analysis for 2 mm and 10 mm. The time step Δt was specified according to the Courant–Friedrichs–Lewy (CFL) criterion and also, it was determined automatically with the help of the Flow-3D software.

Smoothed particle hydrodynamics (SPH) method

The SPH method is described as a technique that includes numerical solutions for fluid dynamics equations using a set of particles and fluid displacement (Dalrymple and Rogers, 2006). One of the most important features of this technique is that SPH is a Lagrangian mesh-free particle method. The Navier–Stokes equations, which are discretized in fluid dynamics problems, can be unified by the physical properties of the particles surrounding each particle position (Vacondio et al., 2012). The average smoothing length is calculated by *Equation 3:*

$$F(r) = \int F(r')\, W(r - r', h)\, (dr') \qquad \text{(Eq.3)}$$

where "W" is the kernel function and "h" is the smoothing length. "W" employed in the smoothing process, can involve several features. It is possible to consider some of these properties as being positive in a specified interaction region. Thus, it maintains gradually decreasing result values owing to the normalization and distance. The function is applied to a set of particles. Also, this function is called as application regions when defined by smoothing length. Therefore, a summation is applied to all particles within these application regions of the kernel (*Eq. 4*) (Ozbulut et al., 2014).

$$F(r_a) \approx \sum_b F(r_b)\, W(r_a - r_b, h) \Delta v_b \qquad \text{(Eq.4)}$$

In *Equation 4*, "a" and "b" symbolize individual particles. Furthermore, Δv_b points out the volume of the neighboring particle "b". As the volume is defined as $\Delta v_b = m_b/\rho_b$, where "m" is the mass and "ρ" is the density of particle, *Equation 4* can be modified as shown in *Equation 5* (Crespo et al., 2015):

$$F(r_a) \approx \sum_b F(r_b)\, \frac{m_b}{\rho_b} W(r_a - r_b, h) \Delta v_b \qquad \text{(Eq.5)}$$

The momentum equation is used to define the acceleration of a particle as a consequence of interaction with a neighboring particle (*Eq. 6*) (Altomare et al., 2015):

$$\frac{dV_a}{dt} - \sum_b m_b \left(\frac{P_b}{{\rho_b}^2} + \frac{P_a}{{\rho_a}^2} + \prod_{ab} \right) \nabla_a W_{ab} + g \qquad \text{(Eq.6)}$$

http://www.aloki.hu ● ISSN 1589 1623 (Print) ● ISSN 1785 0037 (Online)
DOI: http://dx.doi.org/10.15666/aeer/1702_30333047
© 2019, ALÖKI Kft., Budapest, Hungary

In *Equation 6*, v is velocity, P is pressure, m is mass and W_{ab} is the kernel function. The kernel function also depends on the distance between two particles. The term Π_{ab} is called the artificial viscosity (Dominguez et al., 2012). The mass for each particle is constant and the differences in the fluid density are calculated by solving the conservation of mass or continuity equation (*Eq. 7*). Furthermore, Cubic spline was selected as the kernel function type for this study (Cunningham et al., 2014).

$$\frac{d\rho_a}{dt} = \sum_b m_b v_{ab.} \Delta_a W_{ab} \quad \text{(Eq.7)}$$

The pressure value of the flow is calculated using Tait's equation of state as can be seen in *Equation 8* (DualSPHysics Team, 2016):

$$P = b\left[\left(\frac{\rho}{\rho_0}\right)^{\gamma} - 1\right] \quad \text{(Eq.8)}$$

where $\gamma = 7$, $b = c_0{}^2\rho_0/\gamma$, ρ_0: reference density, c_0: the speed of sound. The speed of sound value is calculated from *Equation 9* (Vacondio et al., 2012):

$$c_0 = c(\rho_0) = \sqrt{\left(\frac{\partial P}{\partial p}\right)}\,|_{\rho_0} \quad \text{(Eq.9)}$$

For this study, the Verlet algorithm was used in order to prepare the time stepping process. A variable time-step process was performed, which relies on applying the CFL condition, forcing terms and a viscous diffusion term (Barreiro et al., 2013). Moreover, a boundary condition, where the fluid–boundary interactions can be computed inside the same loops like the fluid particles, is suitable to fulfill due to computational simplicity in this paper. Seeing determine the optimum value of the artificial viscosity, different artificial viscosity values were tested and the optimum value obtained as 0.10. There are many studies in the literature about the use of various artificial viscosity values in the SPH (Gomez-Gesteira et al., 2012; Dominguez et al., 2013; Cunningham et al., 2014; Crespo et al., 2015; Gu et al., 2017; Zhu et al., 2017; Tantekin et al., 2017). SPH parameters can be seen in *Table 1*.

Table 1. *SPH parameters (Turhan et al., 2019)*

Property	Options
Version	DualSPHysics v4.0
Dimension	2D
Type of the kernel function	Cubic spline
Time-stepping	Verlet
Density filter	Shepard filter
Viscosity treatment	Artificial viscosity (α = 0.10)
Equation of state	Tait equation
Boundary conditions (BC)	Dynamic
Distance between particles (dp)	0.001
Smoothing length	1.0
The number of fluid particles	46857

http://www.aloki.hu ● ISSN 1589 1623 (Print) ● ISSN 1785 0037 (Online)
DOI: http://dx.doi.org/10.15666/aeer/1702_30333047
© 2019, ALÖKI Kft., Budapest, Hungary

Results and discussion

In this study, the fluid wave propagation was investigated over a dry bed. Experimental video records were digitized using image processing techniques and the SPH method and RANS equations were used for the numerical models. The propagation of salt water, in a small-scale channel under a sudden dam-break situation, was researched and the variation of fluid depth at four specified locations were examined. In order to show the variation in the free-surface profile of the flow for sudden dam-break flow conditions, the following time values, which represent the initial stages after suddenly lifting the gate, were selected as $t_0 = 0.00$ s, $t_1 = 0.017$ s, $t_2 = 0.083$ s, $t_3 = 0.134$ s, $t_4 = 0.184$ s and $t_5 = 0.234$ s. Moreover, time values, which represent the change of waves reflecting from the wall at the end of the channel, were selected as $t_6 = 1.002$ s, $t_7 = 1.252$ s, $t_8 = 1.670$ s, $t_9 = 2.004$ s, $t_{10} = 2.338$ s and $t_{11} = 2.989$ s (see *Figs. 4* and *5*).

According to the selected time values, the snapshots and level changes in selected locations were compared and the solution sensitivity of the SPH method was analyzed to better understand the unsteady flow behavior. With a sudden lifting of the gate, the fluid starts to move in the downstream direction due to gravitational force. At the initial stages of the propagation, all methods are in good agreement with each other (An et al., 2012; Albano et al., 2014; Bayon et al., 2016; Gu et al., 2017; Zhu et al., 2018). The shock wave front has a parabolic shape for the three methods at t = 0.083 s. At time t = 0.134 s, the wave front is subjected to the deformation and it becomes concave shape. As can be understood from the literature, a similar fluid behavior can be seen in the sudden wave propagation where the fluid is selected as water (Bellos et al., 1992; Stansby et al., 1998; Janosi et al., 2004; Spinewine and Zech, 2007; Ozmen-Cagatay and Kocaman, 2010; Gao et al., 2010; Girolami et al., 2012; Ye et al., 2016; Bayon et al., 2016; Hui et al., 2017; Turhan et al., 2019). However, in the numerical models, the wave front has a convex shape. This difference can be explained by the fact that the experimental channel has minor surface roughness compared to the numerical models.

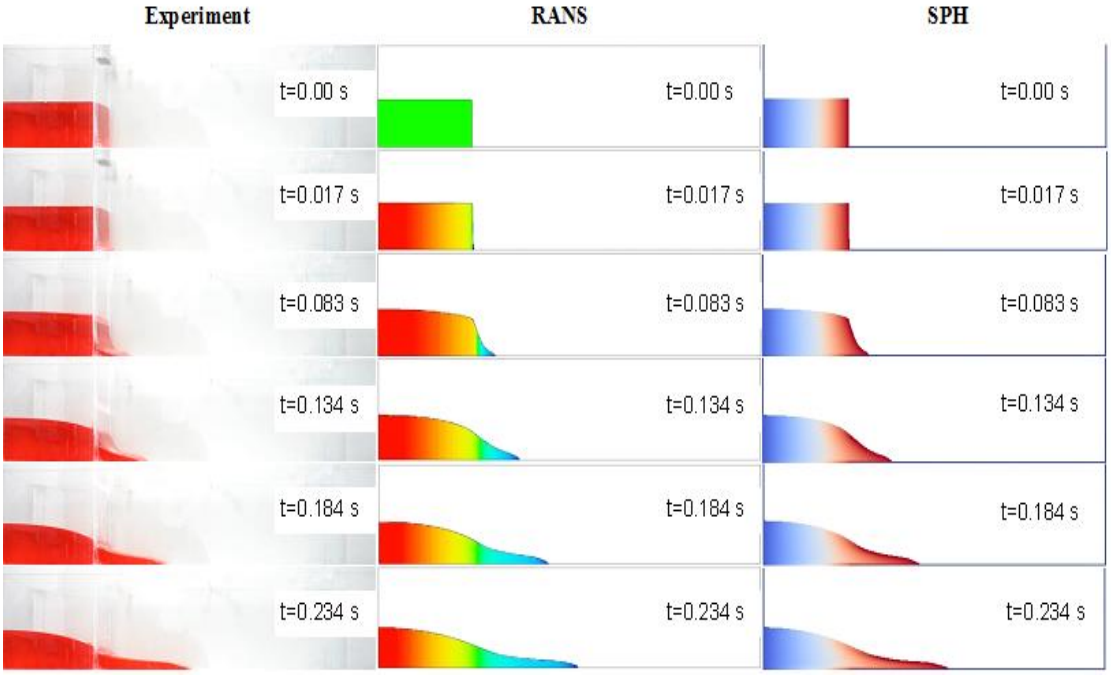

Figure 4. *Evolution of free-surface profiles with time at the initial stages after sudden lifting from t = 0.00 s to t = 0.234 s for experiment, RANS and SPH*

http://www.aloki.hu ● ISSN 1589 1623 (Print) ● ISSN 1785 0037 (Online)
DOI: http://dx.doi.org/10.15666/aeer/1702_30333047
© 2019, ALÖKI Kft., Budapest, Hungary

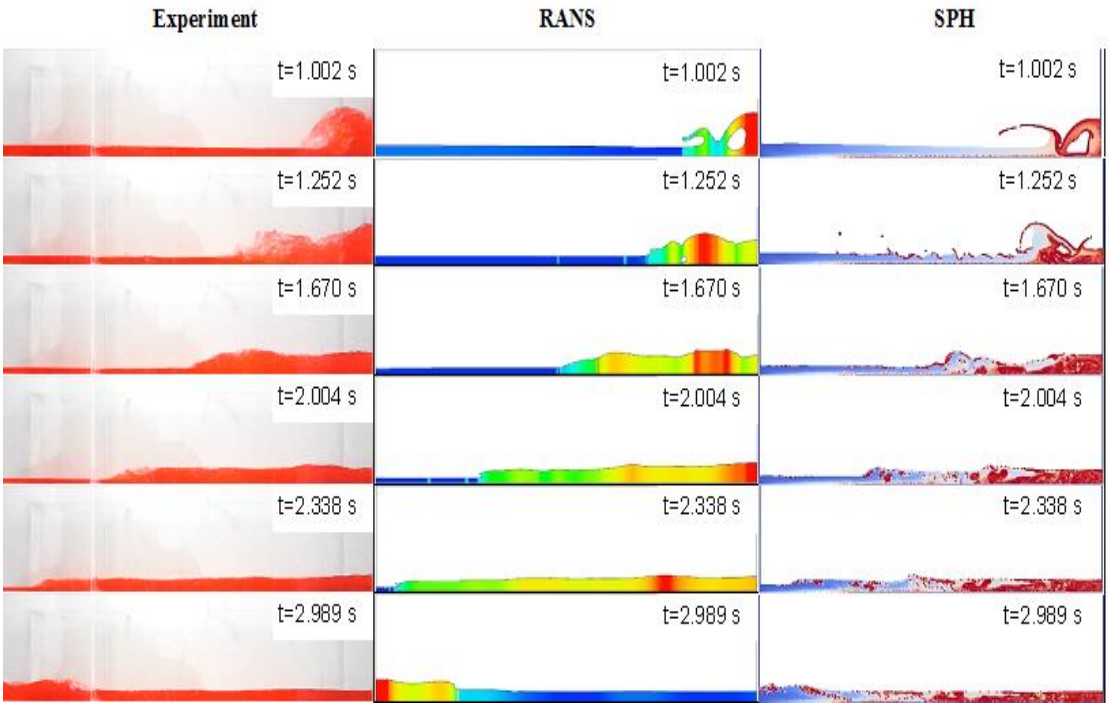

Figure 5. *Evolution of free-surface profiles of reflecting wave with time from t = 1.002 s to t = 2.989 s for experiment, RANS and SPH*

A dam-break flood shock wave over a dry bed can be separated two parts as an initial wave and a dynamic wave after the initial stages (Lauber and Hager, 1998; Chanson, 2005; Ozmen-Cagatay and Kocaman, 2010; Kocaman and Ozmen-Cagatay, 2015; Hui et al., 2017; Turhan et al., 2018). Nsom (2002) defines a convex shape of the wave front for highly viscous fluids. *Figure 5* shows the change in free-surface profiles in the experimental and numerical models for the selected locations in the case of a reflected wave. At t = 1.002 s, the wave rises on the channel surface for a while and the formation of air bubbles is observed in the wave front. When the wave is breaking in the RANS example, the wave jumps to a further point due to disintegration in the SPH. High energy losses in the experiments cause a decrease in the velocity because of the turbulence effect and the fluid level is observed at higher position (Kocaman and Ozmen-Cagatay, 2012; Souders et al., 2013; Rostami and Siosemarde, 2015; Gu et al., 2017; Turhan et al., 2019). At t = 1.252 s, the wave front has a different shape for each methods. In general, RANS results are compatible with the experimental results in terms of the wave front velocity (Ozmen-Cagatay and Kocaman, 2010; Bayon et al., 2016; Heydari and KhoshKonesh, 2016; Hu et al., 2018).

In *Figure 6*, for P1 = 0.15 m, the numerical and experimental results are in good agreement with each other except for T = 20 to 25. For P2 = 0.45 m, except for a few differences, the numerical methods show similar results to each other until T = 15. In the SPH method, between T = 15 and 20, it is seen that the fluid height increased at the initial stages but later, it decreased with time and also it is constant at H = 0.20. However, in the RANS method, the depth was observed to be higher than with the SPH (Turhan et al., 2019). At T = 20, the front of wave became vertical shape for the SPH due to the artificial viscosity coefficient. For P4 = 1.00 m and T = 8 to 10, some fluctuations were seen in the experimental results and the fluid height is lower

http://www.aloki.hu ● ISSN 1589 1623 (Print) ● ISSN 1785 0037 (Online)
DOI: http://dx.doi.org/10.15666/aeer/1702_30333047
© 2019, ALÖKI Kft., Budapest, Hungary

compared to the SPH. Until the end of the propagation, the maximum H value is occurred for T = 10 in the particle method. For P4 = 1 m, the obtained results in RANS and experiments are quite similar except for T = 8 to 15.

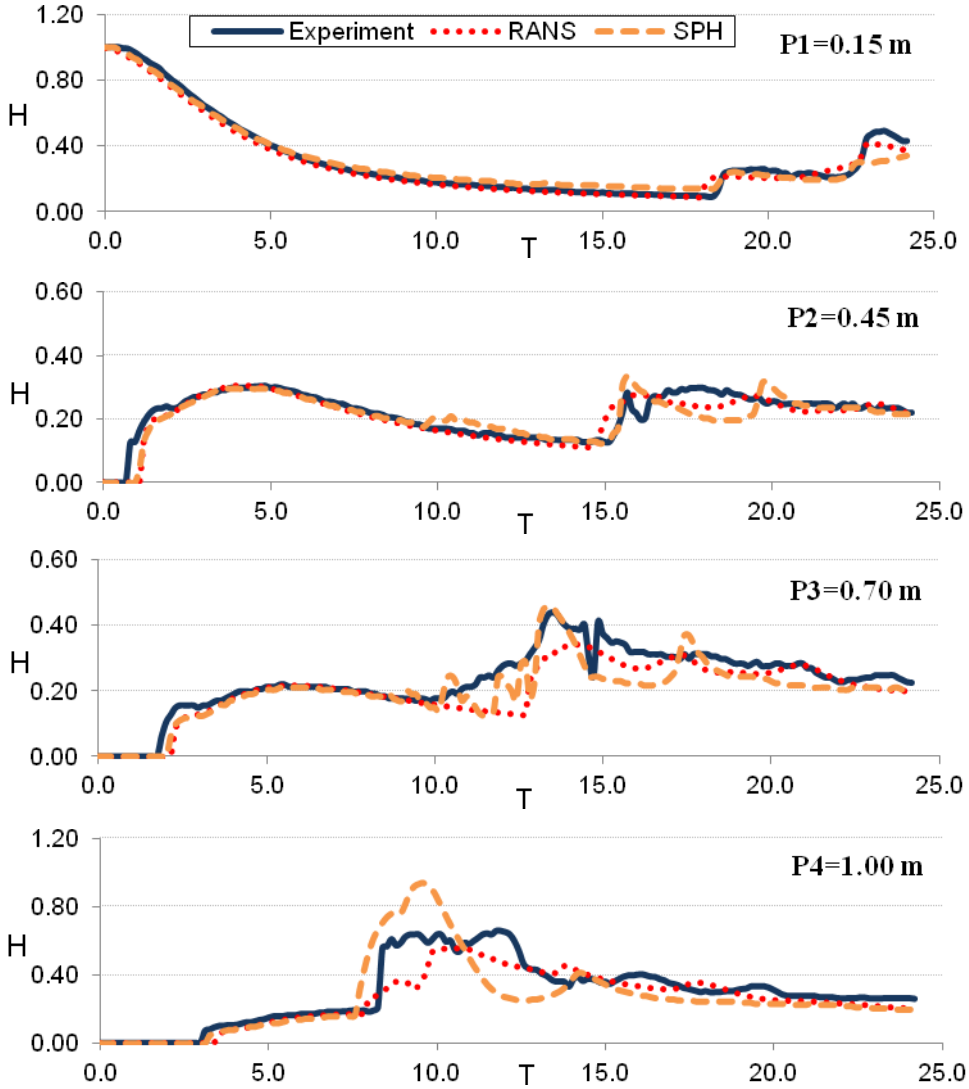

Figure 6. *Flow depth variations with time at P1, P2, P3 and P4*

At T = 10 to 15, the SPH results have been observed to differ from the experimental results. The disintegration of the reflected waves can be mentioned as one of the reasons for the differences due to particle collision in the flow. At T = 25, the experimental and SPH results in the graphs began to meet each other. Furthermore, a more sensitive analysis of the SPH parameters and modeling the wave motion with high-technology-aided computers will greatly increase the capability of the numerical solution (Dominguez et al., 2013; Valdez-Balderas et al., 2013; Turhan, 2017; Akbari, 2018). While the numerical model can generate highly compatible data in the initial stages of the dam-break, the differences between the results for various methods at P4 can be clearly observed due to the wall at the end of the channel. As a result, the propagation of flow in a Newtonian fluid with a different density, such as salt water for this study, can

http://www.aloki.hu ● ISSN 1589 1623 (Print) ● ISSN 1785 0037 (Online)
DOI: http://dx.doi.org/10.15666/aeer/1702_30333047
© 2019, ALÖKI Kft., Budapest, Hungary

yield similar results with the cases in which water was used as a fluid in the initial stages for both experimental and numerical results.

In addition, the reflected waves after hitting the wall become more vertical shape in the propagation of water and the formation of bubbles on the front face of the wave draws more attention (Zhu et al., 2018; Turhan et al., 2018). For fluid propagation, wave breaking, jet and bubble formations can be observed for some time due to the turbulence effect (Janosi et al., 2004; Li et al., 2013; Hu et al., 2018; Liu et al., 2018).

Conclusion

Difficulties in the application of dam-break flow problems require from utilizing numerical methods because of rough real case conditions. In recent years, the advances in computer technology have enabled computer-aided software programs to easily solve these problems. Therefore, the validation of numerical methods can considerably provide to test the sensitivity of the experimental solutions. In this study, the dam-break flow problem, in which the liquid is salt water, was investigated both experimentally and numerically over a dry bed to gain a better understanding of the effects of different density fluid. According to the results, the values obtained from both numerical methods and experiments are close to each other, but when the turbulence effect is high, the free-surface profiles and graphs show some differences. In these periods, major changes are observed using the SPH method. However, RANS results are in good agreement with the experiments. The artificial viscosity and particle approach in the SPH cause differences in the results in terms of profiles and graphs. The use of artificial viscosity in the SPH increases the differences between the results in each case. Although the results obtained from the SPH is usually considered to be good in agreement with the results obtained from other methods, studies performing more sensitive analyses can make greater contributions with more consistency. It can be stated that SPH, a mesh-free particle based Lagrange method, may be adopted as a useful numerical method for solving complex open channel flow problems.

As further studies, force and velocity measurements in dam-break problems, the effect of channel base roughness and channel slope on flow characteristics can be examined. In addition, several artificial viscosity and smoothing length values can be investigated to observe the performance of the numerical model under different parameters.

Acknowledgements. This study was supported by Çukurova University Scientific Research Projects Unit with the project code of *FDK-2015-4887*. The authors would like to thank Çukurova University Scientific Research Projects Unit on account of providing and helping in this research.

REFERENCES

[1] Akbari, H. (2018): Evaluation of incompressible and compressible SPH methods in modeling dam break flows. – International Journal of Coastal & Offshore Engineering 2(1): 45-57.

[2] Albano, R., Mirauda, D., Sole, A., Amicarelli, A., Agate, G., Taramasso, A. C. (2014): Experimental validation of a 3D SPH model for the simulation of a dam-break event involving multiple fixed and mobile bodies. – 7th WSEAS International Conference on Engineering Mechanics, Structures, Engineering Geology, Italy 30-37.

http://www.aloki.hu ● ISSN 1589 1623 (Print) ● ISSN 1785 0037 (Online)
DOI: http://dx.doi.org/10.15666/aeer/1702_30333047
© 2019, ALÖKI Kft., Budapest, Hungary

[3] Albano, R., Sole, A., Mirauda, D., Adamowski, J. (2016): Modelling large floating bodies in urban area flash-floods via a smoothed particle hydrodynamics model. – J. Hydrol. 541: 344-358.
[4] Altomare, C., Crespo, A. J. C., Dominguez, J. M., Gomez-Gesteira, M., Suzuki, T., Verwaest, T. (2015): Applicability of smoothed particle hydrodynamics for estimation of sea wave impact on coastal structures. – Coastal Engineering 96: 1-12.
[5] Amaral, S., Viseu, T., Bento, A. M., Jonatas, R., Calderia, L., Cardoso, R., Ferreira, R. M. L. (2016): Experiments on earths dam breaching, monitoring instrumentation and methods. – 10º Congresso Nacionalde Mecânica Experimental (CNME), Lisbon, Portugal 1-12.
[6] An, S., Julien, P. Y., Venayagamoorthy, S. K. (2012): Numerical simulation of particle-driven gravity currents. – Environ Fluid Mech. 12: 495-513.
[7] Ancey, C., Cochard, S. (2009): The dam-break problem for erschel-Bulkley viscoplastic fluids down steep flumes. – Journal of Non-Newtonian Fluid Mech. 158: 18-35. DOI: 10.1016/j.jnnfm.2008.08.008.
[8] Aureli, F., Maranzoni, A., Mignosa, P., Ziveri, C. (2011): An image processing technique for measuring free surface of dam break flows. – Exp Fluids 50: 665-675. DOI: 10.1007/s00348-010-0953-6.
[9] Aureli, F., Dazzi, S., Maranzoni, A., Mignosa, P., Vacondio, R. (2014): Experimental and numerical evaluation of the force due to the impact of a dam-break wave on a structure. – Advances in Water Resources 76: 29-42.
[10] Barreiro, A., Crespo, A. J. C., Dominguez, J. M., Gomez-Gesteira, M. (2013): Smoothed particle hydrodynamics for coastal engineering problems. – Computers and Structures 120: 96-106.
[11] Bayon, A., Valero, D., Garcia-Bartual, R., Valles-Moran, F. J., Lopez-Jimenez, P. A. (2016): Performance assessment of OpenFOAM and FLOW-3D in the numerical modeling of a low Reynolds number hydraulic jump. – Environmental Modelling & Software 80: 322-335.
[12] Bellos, V., Soulis, J. V., Sakkas, J. G. (1992): Experimental investigation of two-dimensional dam-break induced flows. – Journal of Hydraulic Research 30(1): 47-63.
[13] Bukreev, V. I., Gusev, A. (2005): Initial stage of the generation of dam-break waves. – Doklady Physics 50(4): 200-203.
[14] Chanson, H. (2005): Analytical solution of dam break wave with flow resistance application to tsunami surges. – XXXI. IAHR Congress, September 12-16, Seoul, Korea, 3341-3356.
[15] Chen, A. S., Hsu, M. H., Chen, T. S., Chang, T. J. (2005): An integrated inundation model for highly developed urban areas. – Water Sci. Technol. 51: 221-229.
[16] Crespo, A. J. C., Dominguez, J. M., Rogers, B. D., Gomez-Gesteira, M., Longshaw, S., Canelas, R., Vacondio, R., Barreiro, A., Garcia-Feal, O. (2015): DualSPHysics: Open-source parallel CFD solver based on smoothed particle hydrodynamics (SPH). – Computer Physics Communications 187: 204-216. http://dx.doi.org/10.1016/j.cpc.2014.10.004.
[17] Cunningham, L. S., Rogers, B. D., Pringgana, G. (2014): Tsunami wave and structure interaction: an investigation with smoothed-particle hydrodynamics. – Engineering and Computational Mechanics 167(3): 126-138.
[18] Dalrymple, R., Rogers, B. (2006): Numerical modeling of water waves with the SPH method. – Coastal Engineering 53: 141-147. DOI: 10.1016/j.coastaleng.2005.10.004.
[19] Dominguez, J. M., Crespo, A. J. C., Gomez-Gesteira, M. (2012): Optimization strategies for CPU and GPU implementations of a smoothed particle hydrodynamics method. – Computer Physics Communications 184: 617-627.
[20] Dominguez, J. M., Crespo, A. J. C., Valdez-Balderas, D., Rogers, B. D., Gomez-Gesteira, M. (2013): New multi-GPU implementation for smoothed particle hydrodynamics on heterogeneous clusters. – Computer Physics Communications 184: 1848-1860.

http://www.aloki.hu ● ISSN 1589 1623 (Print) ● ISSN 1785 0037 (Online)
DOI: http://dx.doi.org/10.15666/aeer/1702_30333047
© 2019, ALÖKI Kft., Budapest, Hungary

[21] DualSPHysics Team (2016): User Guide for DualSPHysics Code. – User Guide 140.
[22] Flow Science Inc (2017): Flow-3D user manual. – Flow Science, Santa Fe, NM.
[23] Furuya, M., Oka, Y., Satoh, M., Lo, S., Arai, T. (2014): Advanced computational methods and experiments in heat transfer. – XIII. WIT Transactions on Engineering Sciences 83: 363-374. DOI: 10.2495/HT140321.
[24] Gao, Z., Vassalos, D., Gao, Q. (2010): Numerical simulation of water flooding into a damaged vessel's compartment by the volume of fluid method. – Ocean Engineering 37: 1428-1442.
[25] Gingold, R. A., Monaghan, J. J. (1977): Smoothed particle hydrodynamics: theory and application to non-spherical stars. – Monthly Notices of the Royal Astronomical Society 181: 375-389.
[26] Girolami, L., Hergault, V., Vinay, G., Wachs, A. (2012): A three-dimensional discrete-grain model for the simulation of dam-break rectangular collapses: comparison between numerical results and experiments. – Granular Matter 14: 381-392.
[27] Gomez-Gesteira, M., Rogers, B. D., Crespo, A. J. C., Dalrypmle, R. A., Narayanaswamy, M., Dominguez, J. M. (2012): SPHysics - development of a free-surface fluid solver - Part 1: Theory and formulations. – Computer & Geosciences 48: 289-299.
[28] Gu, S., Zheng, X., Ren, L., Xie, H., Huang, Y., Wei, J., Shao, S. (2017): SWE-SPHysics simulation of dam break flows at South-Gate Gorges Reservoir. – Water 9: 387-406.
[29] Heydari, M., KhoshKonesh, A. (2016): The comparison of the performance of Prandtl, mixing length, turbulence kinetic energy, K-e, RNG and LES turbulence models in simulation of the positive wave motion caused by dam break on the erodible bed. – Indian Journal of Science and Technology 9(7): 1-33. doi: 10.17485/ijst/2016/v9i7/87856.
[30] Hu, H., Zhang, J., Li, T. (2018): Dam-break flows: comparison between Flow-3D, MIKE 3 FM, and analytical solutions with experimental data. – MDPI, Applied Sciences 8(12): 2456-2480. DOI: 10.3390/app8122456.
[31] Hui, L., Haijiang, L., Liheng, G., Senxun, L. (2017): Experimental study on the dam-break hydrographs at the gate location. – J. Ocean Univ. China 16: 697-702.
[32] Janosi, I. M., Jan, D., Szabo, K. G., Tel, T. (2004): Turbulent drag reduction in dam-break flows. – Experiments in Fluids 37: 219-229.
[33] Karaer, F., Koparal, A. S., Tombul, M. (2018): Environmental risk determination of flood in Porsuk River Basin via one-dimensional modelling. – Applied Ecology and Environmental Research 16(4): 4969-4983. http://dx.doi.org/10.15666/aeer/1604_49694983.
[34] Kocaman, S., Guzel, H. (2011): Numerical and experimental investigation of dam-break wave on a single building situated downstream. – Proceedings of International Balkans Conference on Challenges of Civil Engineering, BCCE, EPOKA University, Tirana, Albania.
[35] Kocaman, S., Ozmen-Cagatay, H. (2012): The effect of lateral channel contraction on dam break flows: Laboratory experiment. – Journal of Hydrology 432-433: 145-153.
[36] Kocaman, S., Ozmen-Cagatay, H. (2015): Investigation of dam-break induced shock waves impact on a vertical wall. – Journal of Hydrology 525: 1-12. doi: 10.1016/j.jhydrol.2015.03.040.
[37] Kunugi, T., Hara, K., Nagatake, T., Kawara, Z. (2013): Reconsideration of scaling measure for liquid-column break problem. – AIP Conference Proceedings 1547(1): 280-289.
[38] Lauber, G., Hager, W. H. (1998): Experiments to dam break wave: horizontal channel. – Journal of Hydraulic Research 36(3): 291-308.
[39] Lee, K. E., Shahabudin, S. M., Mokhtar, M., Choy, Y. K., Goh, T. L., Simon, N. (2018): Sustainable water resources management and potential development of multi-purpose dam: the case of Malaysia. – Applied Ecology and Environmental Research 16(3): 2323-2347. http://dx.doi.org/10.15666/aeer/1603_23232347.

http://www.aloki.hu ● ISSN 1589 1623 (Print) ● ISSN 1785 0037 (Online)
DOI: http://dx.doi.org/10.15666/aeer/1702_30333047
© 2019, ALÖKI Kft., Budapest, Hungary

[40] Li, G., Oka, Y., Furuya, M., Kondo, M. (2013): Experiments and MPS analysis of stratification behavior of two immiscible fluids. – Nuclear Engineering and Design 265: 210-221.
[41] Liu, G. R., Liu, M. B. (2003): Smoothed Particle Hydrodynamics: A Meshfree Particle Method. – World Scientific Publishing, Singapore.
[42] Liu, W., Wang, B., Chen, Y., Wu, C., Liu, X. (2018): Assessing the analytical solution of one-dimensional gravity wave model equations using dam-break experimental measurements. – Water, MDPI 10(9): 1261.
[43] Lobosvky, L., Botia-Vera, E., Castellana, F., Mas-Soler, J., Souto-Iglesias, A. (2014): Experimental investigation of dynamic pressure loads during dam break. – Journal of Fluids and Structures 48: 407-434. doi.org/10.1016/j.jfluidstructs.2014.03.009.
[44] Lucy, L. B. (1977): A numerical approach to the testing of the fission hypothesis. – Astronomical Journal 82: 1013-1024.
[45] Luo, Z., Wu, Q., Zhang, L. (2017): Parallel simulation of dam-break flow by OpenMP-based SPH method. – IOP Conf. Series: Journal of Physics: Conf. Series 96: 1-10.
[46] Miao, J., Chen, J., Zhou, J. (2011): Two-dimensional Vertical SPH Method for Dambreak Flow Simulation. – International Conference on Multimedia Technology, 6-28 July 2011, Hangzhou, China, pp. 1384-1386.
[47] Mohapatra, P. K., Bhallamudi, S. M. (1996): Computation of a dam-break flood wave in channel transitions. – Advances in Water Resources 19(3): 181-187.
[48] Nsom, B. (2002): Horizontal Viscous Dam-Break Flow: Experiments and Theory Journal of Hydraulic Engineering. – Journal of Hydraulic Engineering 128(5): 543-546.
[49] Oertel, M., Bung, D. B. (2012): Initial stage of two-dimensional dam-break waves laboratory versus VOF. – Journal of Hydraulic Research 50(1): 89-97. DOI: 10.1080/00221686.2011.639981.
[50] Ozbulut, M., Yıldız, M., Goren, O. (2014): A numerical investigation into the correction algorithms for SPH method in modeling violent free surface flows. – International Journal of Mechanical Sciences 79: 56-65. http://dx.doi.org/10.1016/j.ijmecsci.2013.11.021.
[51] Ozdil, N. F., Tantekin, A., Turhan, E. (2017): A numerical study: unsteady flow propagation using two different methods. – 3rd Conference on Advances in Mechanical Engineering, 19th to 21st December, Yildiz Technical University, pp. 404-409.
[52] Ozmen-Cagatay, H., Kocaman, S. (2010): Dam-break flows during initial stage using SWE and RANS approaches. – Journal of Hydraulic Research 48(5): 603-611. DOI: 10.1080/00221686.2010.507342.
[53] Ozmen-Cagatay, H., Kocaman, S., Guzel, H. (2014): Investigation of dam-break flood waves in a dry channel with a hump. – Journal of Hydro-Environment Research 8: 304-315. doi: 10.1016/j.jher.2014.01.005.
[54] Ritter, A. (1892): Die Fortpflanzung der Wasserwellen. – Vereine Deutscher Ingenieure Zeitschrift 36(2): 947-954.
[55] Robb, D. M., Vasquez, J. A. (2015): Numerical simulation of dam-break flows using depth-averaged hydrodynamic and three-dimensional CFD models. – 22nd Canadian Hydrotechnical Conference, Water for Sustainable Development: Coping with Climate and Environmental Changes, Montreal, Canada, pp. 1-11.
[56] Rostami, M., Siosemarde, M. (2015): Human life saving by simulation of dam break using Flow-3D (A case study: Upper Gotvand Dam). – Trends in Life Sciences, Dama International 4(3): 308-316.
[57] Shakibaeinia, A., Jin, Y. C. (2011): A mesh-free particle model for simulation of mobile-bed dam break. – Advances in Water Resources 34: 794-807. DOI: 10.1016/j.advwatres.2011.04.011.
[58] Souders, D., Kariya, J., Burnham, J. (2013): Validation of a hybrid 3-dimensional and 2-dimensional numerical flow modeling technique for an instantaneous dam-break. – Proceedings of Flow-3D Conference, September 19-20, 2013 Chicago, IL, pp. 1-7.

http://www.aloki.hu ● ISSN 1589 1623 (Print) ● ISSN 1785 0037 (Online)
DOI: http://dx.doi.org/10.15666/aeer/1702_30333047
© 2019, ALÖKI Kft., Budapest, Hungary

[59] Spinewine, B., Zech, Y. (2007): Small-scale laboratory dam-break waves on movable beds. – Journal of Hydraulic Research 45: 73-86.
[60] Stansby, P. K., Chegini, A., Barnes, T. C. D. (1998): The initial stages of dam-break flow. – J. Fluid Mech. 374: 407-424.
[61] Stoker, J. J. (1957): Water Waves. – Interscience Publishers, Wiley, New York, pp. 333-341.
[62] Tantekin, A., Ozdil, N. F., Turhan, E. (2017) The investigation of unsteady flow propagation using different numerical methods based on particle and grid approach. – 4th International Conference on Pure and Applied Sciences: Renewable Energies, 23-25 November, Istanbul, Turkey, pp. 189-189.
[63] Turhan, E. (2017): The investigation of dam-break flow using with experimental and Smoothing Particle Hydrodynamics (SPH) methods. – PhD Thesis, Cukurova University, Institute of Natural and Applied Sciences, Adana.
[64] Turhan, E., Dal, K., Ozmen-Cagatay, H., Kocaman, S. (2018): An experimental and numerical study of dam-break flow problem with different density fluid. – 5th International Dam Safety Symposium, Istanbul, pp. 1426-1437.
[65] Turhan, E., Ozmen-Cagatay, H., Kocaman, S. (2019): Experimental and numerical investigation of shock wave propagation due to dam-break over wet channel. – Polish Journal of Environmental Studies 28(6): 1-24. DOI: 10.15244/pjoes/92824.
[66] Vacondio, R., Rogers, B. D., Stansby, P. K. (2012): Accurate particle splitting for smoothed particle hydrodynamics in shallow water with shock capturing. – Int. J. Numer. Meth. Fluids 69: 1377-1410. DOI: 10.1002/fld.2646.
[67] Valdez-Balderas, D., Dominguez, J. M., Rogers, B. D., Crespo, A. J. C. (2013): Towards accelerating smoothed particle hydrodynamics simulations for free surface flows on multi-GPU clusters. – J. Parallel Distrib. Comput. 73: 1483-1493.
[68] Vischer, D. L., Hager, W. H. (1998): Dam Hydraulics. – John Willey and Sons Ltd., UK, pp. 271-304.
[69] Wilcox, D. C. (2000): Turbulence Modelling for CFD. – DCW Industries, Inc., La Canada, CA.
[70] Xie, H., Gu, S. (2017): Dam Break Flow Simulations and Flooding Wave Analysis at South-Gate Gorges Reservoir Dam; Engineering Report. – Flood Control Institute Qinghai, China.
[71] Yang, X., Wei-lin, X., Shu-jing, L., Hua-yong, C., Nai-wen, L. (2011): Experimental study of dam-break flow in cascade reservoirs with steep bottom slope. – Journal of Hydrodynamics 23(4): 491-497.
[72] Ye, Z., Zhao, X., Deng, Z. (2016): Numerical investigation of the gate motion effect on a dam break flow. – J Mar Sci Technol 21: 579-591. DOI: 10.1007/S00773-016-0374-1.
[73] Yenigun, K., Ulgen, M. U., Aydogdu, M. H., Yenigun, I. (2016): Investigation of the maximum flow trends and their impact on risk levels of spillways. – Applied Ecology and Environmental Research 14(4): 589-606.
[74] Yıldırım, K. S., Ince, C., Kalaycı, T. E. (2003): Image Processing Techniques Notes. – Ege University, Department of Computer Engineering, Izmir.
[75] Zhu, G. X., Zou, L., Chen, Z., Wang, A. M., Liu, M. B. (2018): An improved SPH model for multiphase flows with large density ratios. – Int J Numer Meth Fluids 86: 167-184.

http://www.aloki.hu ● ISSN 1589 1623 (Print) ● ISSN 1785 0037 (Online)
DOI: http://dx.doi.org/10.15666/aeer/1702_30333047
© 2019, ALÖKI Kft., Budapest, Hungary